

# Role of $T=0$ pairing in Gamow-Teller states in $N=Z$ nuclei

C. L. Bai<sup>a</sup>, H. Sagawa<sup>b,c</sup>, M. Sasano<sup>c</sup>, T. Uesaka<sup>c</sup>, K. Hagino<sup>d</sup>, H. Q. Zhang<sup>e</sup>, X. Z. Zhang<sup>e</sup>, F. R. Xu<sup>f</sup>

<sup>a</sup>Department of Physics, Sichuan University, Chengdu 610065, China

<sup>b</sup>Center for Mathematics and Physics, University of Aizu, Aizu-Wakamatsu, 965-8580 Fukushima, Japan

<sup>c</sup>RIKEN, Nishina Center, Wako, 351-0198, Japan

<sup>d</sup>Department of Physics, Tohoku University, Sendai 980-8578, Japan

<sup>e</sup>China Institute of Atomic Energy, Beijing 102413, China

<sup>f</sup>School of Physics, Peking University, Beijing 100871, China

## Abstract

Gamow-Teller (GT) states in  $N=Z$  nuclei with the mass number  $A$  from 48 to 64 are studied by using Hartree-Fock-Bogoliubov + quasi-particle random phase approximation (HFB+QRPA) with Skyrme interactions. The isoscalar spin-triplet ( $T=0, S=1$ ) pairing interaction is taken into account in QRPA calculations. It is found in the context of  $SU(4)$  symmetry in the spin-isospin space that the GT strength of lower energy excitations is largely enhanced by the  $T=0$  pairing interaction which works cooperatively with the  $T=1$  pairing interaction in the ground state. A two-peaked structure observed recently in  $(p, n)$  reaction on  $^{56}\text{Ni}$  can be considered as a manifestation of the role of  $T=0$  pairing in the GT collective states.

**Keywords:**

Gamow Teller states,  $T=0$  pairing interaction,  $SU(4)$  supermultiplet

The most prominent evidence of pairing correlation in nuclei is found in the odd-even staggering in binding energies and the gap in the excitation spectrum of even-even nuclei in contrast to the compressed quasi-particle spectrum in odd- $A$  nuclei [1, 2, 3]. There are also dynamical effects of pairing correlations seen in the moment of inertia associated with nuclear rotation and large amplitude collective motion [3, 4, 5]. The Hartree-Fock (HF)+BCS method and Hartree-Fock-Bogoliubov (HFB) method have been commonly used to study the ground state properties of superfluid nuclei in a broad mass region [6, 7, 8, 9]. For the study of excited spectra, quasi-particle random phase approximation (QRPA) has often been adopted as a basic method [10, 11, 12, 13].

The strong attraction between nucleons is the basic ingredient for the pairing correlations. So far, the pairing interactions of like-nucleons with the isovector spin-singlet ( $T=1, S=0$ ) channel has been mainly discussed. In fact, the attraction between protons and neutrons is even stronger in the isoscalar spin-triplet ( $T=0, S=1$ ) channel [14], which gives rise to the deuteron bound state. However the role of  $T=0$  pairing is limited in nuclei because of large imbalance between neutron and proton numbers, and also the two-body spin-orbit interaction which breaks the  $S=1$  pair more effectively than the  $S=0$  pair [4, 15, 16]. Nevertheless, the isoscalar pairing causes extra binding energies in nuclei with  $N=Z$  and has been considered as one of the origins of the Wigner energy [17].

Gamow-Teller (GT) states have been studied both experimentally and theoretically intensively in the last three decades. Many interesting nuclear structure information has been re-

vealed by these studies, for example, the quenching of sum rule strength [18] and the role of GT strength in the astrophysical processes such as neutrino-nucleus reactions [19]. Because of recent development of modern radioactive beam accelerator, it becomes feasible to observe GT states in exotic nuclei near the proton and neutron drip lines. Recently, the GT transition strength was studied in a  $N=Z$  nucleus  $^{56}\text{Ni}$  which has an important impact on late stellar evolution through electron capture and  $\beta$  decay [20]. Although the collective GT state is mainly built of charge exchange particle-hole excitations, the low-lying strength responsible for  $\beta$  decay involves neutron-proton ( $np$ ) particle-particle type excitations which could be sensitive to the  $T=0$  pairing interaction [10, 21]. Intuitively, the low-energy GT excitations will be enhanced by the following mechanism: the  $T=1$  pairing correlation provides partially occupied proton and the neutron orbitals near the Fermi surface. These orbitals will accept the additional proton excitations from the neutron orbits with the same orbital  $l$  quantum number. Then, these ( $np$ ) pair interacts through the  $T=0$  pairing interaction and enhances GT strength. These physical mechanisms may implement the super-allowed GT transition between the same multiplet members of  $SU(4)$  symmetry in the spin-isospin space which never happened when a neutron orbital is completely full and the corresponding proton one is empty. In this letter, we study GT states in several  $N=Z$  nuclei focusing on the cooperative role of  $T=1$  and  $T=0$  pairing interactions in the GT transitions. In Refs. [23, 24, 25], we applied successfully the self-consistent HF+RPA model to calculate spin and isospin dependent excitations in several closed shell nuclei. As an extension to open shell nuclei, the HFB+QRPA method is used to calculate GT states with realistic Skyrme interactions.

Email address: sagawa@u-aizu.ac.jp (H. Sagawa)

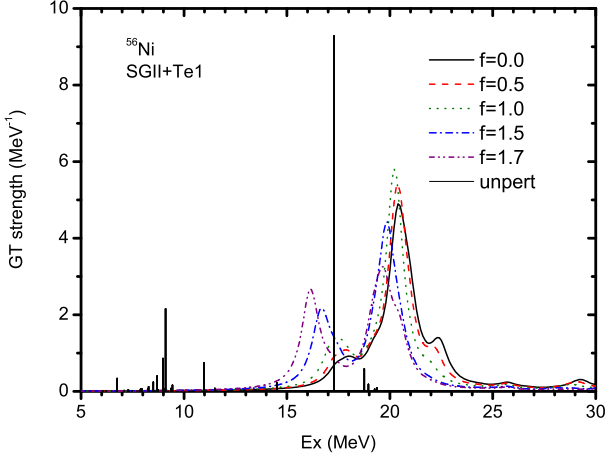


Figure 1: (Color online) Gamow-Teller strength in  $^{56}\text{Ni}$  obtained by HFB+QRPA calculations with the Skyrme interaction SGII+Te1. The excitation energy is referred to the ground state of  $^{56}\text{Ni}$ . The T=0 pairing interaction is included in QRPA changing the coupling constant  $f$  from  $f=0.0, 0.5, 1.0, 1.5$  and  $1.7$  in Eq. (2). The solid lines show the unperturbed strength without RPA correlations. The QRPA strength is smoothed out by a Lorentzian function with a width  $\Gamma = 1$  MeV

The density dependent contact pairing interactions are adopted for both T=1 and T=0 channels,

$$V_{T=1}(\mathbf{r}_1, \mathbf{r}_2) = V_0 \frac{1 - P_\sigma}{2} \left( 1 - \frac{\rho(\mathbf{r})}{\rho_0} \right) \delta(\mathbf{r}_1 - \mathbf{r}_2), \quad (1)$$

$$V_{T=0}(\mathbf{r}_1, \mathbf{r}_2) = f V_0 \frac{1 + P_\sigma}{2} \left( 1 - \frac{\rho(\mathbf{r})}{\rho_0} \right) \delta(\mathbf{r}_1 - \mathbf{r}_2), \quad (2)$$

where  $\mathbf{r} = (\mathbf{r}_1 + \mathbf{r}_2)/2$  and  $\rho_0$  is the saturation density taken to be  $\rho_0 = 0.16 \text{ fm}^{-3}$ . The strength of T=1 pairing is determined to reproduce the average odd-even mass staggering gap  $\Delta^{(3)} = 12/A^{1/3} \text{ MeV}$  in N=28 region to be  $V_0 = -550 \text{ MeV} \cdot \text{fm}^3$ . We solve firstly the HFB equations in coordinate space with a large radial mesh extending up to 20 fm with a step of 0.05 fm. In QRPA, we take into account all the states up to 180 MeV excitation energy which have the occupation probabilities more than  $v^2 = 10^{-6}$ . The T=0 pairing is changed from null pairing to strong pairing limit taking the factor  $f$  from  $f=0.0, 0.5, 1.0, 1.5$  and  $1.7$ . The  $f=1.7$  is the maximum value to avoid the spin-isospin instability of the ground state of  $^{56}\text{Cu}$ .

The GT transition involves both the spin and isospin operators as

$$\hat{O}(GT) = \sum_i \sigma(i) t_\pm(i) \quad (3)$$

for spin-flip and isospin-flip excitations. The calculated GT states in  $^{56}\text{Ni}$  for  $t_-$  channel are shown in Fig.1 where the interaction SGII+Te1 [24, 25] is used for HF mean field and particle-hole interactions. The unperturbed strengths shown by solid straight lines have two groups at  $E_x=9$  MeV and 17 MeV. The QRPA results without T=0 pairing shown by the black curve have the main peak around 20.4 MeV together with a small peak at 18.0 MeV. When the T=0 pairing strength is introduced, the global GT strength is shifted to lower energy. At the same time, the GT strength of lower peak is increased and absorbs

Table 1: Amplitudes of main ( $np$ ) particle-hole and particle-particle type configurations of GT states in  $^{56}\text{Ni}$ . The QRPA calculations are performed without and with the T=0 pairing interaction in the cases of  $f = 0$  and  $f = 1.5$ , respectively. The Skyrme interaction T21 is used for HF and p-h matrix calculations. The abbreviations  $B$  and  $C$  correspond to the GT reduced matrix element and the normalization factor defined in Eqs. (4) and (5), respectively. The excitation energy  $E_x$  is given in unit of MeV .

$^{56}\text{Ni}$ $f = 0$					
$E_x$	B(GT)	$\nu(v_\nu^2)$	$\pi(v_\pi^2)$	B	C
17.5	1.41	$2p_{3/2}(0.20)$	$2p_{3/2}(0.21)$	0.358	0.127
		$1f_{7/2}(0.69)$	$1f_{5/2}(0.09)$	-0.229	0.006
		$1f_{7/2}(0.69)$	$1f_{7/2}(0.67)$	1.341	0.802
18.3	1.49	$2p_{1/2}(0.10)$	$2p_{3/2}(0.21)$	0.260	0.153
		$2p_{3/2}(0.20)$	$2p_{1/2}(0.11)$	0.846	0.740
21.3	7.88	$1f_{7/2}(0.69)$	$1f_{5/2}(0.09)$	2.48	0.742
$S_-(\text{GT})=18.28$					
$^{56}\text{Ni}$ $f = 1.5$					
$E_x$	B(GT)	$\nu(v_\nu^2)$	$\pi(v_\pi^2)$	B	C
16.6	4.82	$2p_{3/2}(0.20)$	$2p_{1/2}(0.11)$	-0.203	0.049
		$2p_{3/2}(0.20)$	$2p_{3/2}(0.21)$	-0.682	0.491
		$1f_{7/2}(0.69)$	$1f_{5/2}(0.09)$	-0.237	0.007
		$1f_{7/2}(0.69)$	$1f_{7/2}(0.67)$	-0.790	0.339
20.5	4.10	$1f_{7/2}(0.69)$	$1f_{5/2}(0.09)$	-1.900	0.437
$S_-(\text{GT})=14.75$					

the major strength when the T=0 pairing is stronger than T=1 ( $f \geq 1$ ).

The HFB+QRPA results for  $t_-$  channel are shown in Fig. 2 for  $^{48}\text{Cr}$ ,  $^{56}\text{Ni}$  and  $^{64}\text{Ge}$ . The interaction T21 [26] is used for HF mean field and particle-hole interactions. When the T=0 pairing strength is introduced, the global GT strength is shifted to lower energy. At the same time, the increase of lower energy peak is always seen in the three nuclei as the T=0 pairing becomes stronger. As a systematic trend, the lighter the mass is the larger the lower energy GT peak is. In the two nuclei  $^{56}\text{Ni}$  and  $^{64}\text{Ge}$ , the double peak structure can be seen even in the strong T=0 pairing limit at  $f = 1.7$ . On the contrary, in  $^{48}\text{Cr}$ , the higher energy peak is almost disappeared in the case of  $f = 1.7$ . We found this trend also in  $^{44}\text{Ti}$  in which the higher energy peak is very small and is not seen in the case of  $f \geq 1.5$ .

The experimental data of  $^{56}\text{Ni}$  show two peaks at 18.7 and 20.8 MeV [20], as is shown in the middle panel of Fig. 2. The calculated results for  $^{56}\text{Ni}$  with T=0 pairing of  $f = 1.0$  and  $f = 1.5$  give almost the identical peak energy to the observed one for the higher excitation peak. On the other hand, the calculated lower peak is 2 MeV lower than the experimental one in energy.

Main configurations of dominant GT states in  $^{56}\text{Ni}$  are tabulated in Table 1 without and with the T=0 pairing interaction ( $f = 0.0$  and  $f = 1.5$ ), respectively. In Table 1, the value B corresponds to the GT reduced matrix element

$$B = (Xu_\pi v_\nu - Yu_\nu v_\pi) \langle \pi || \hat{O}(GT) || \nu \rangle \quad (4)$$

with the operator Eq. (3), and the value

$$C = X^2 - Y^2, \quad (5)$$

is the normalization factor where  $X$  and  $Y$  are QRPA amplitudes. The dominant configurations are only listed in Table 1. Without the  $T=0$  pairing, the main configuration of higher excitation is a particle-hole type ( $1f_{7/2}^{\nu}, 1f_{5/2}^{\pi}$ ) excitation referring to the configuration of fully occupied  $1f_{7/2}$  proton and neutron orbits, while that of lower energy has particle-particle type ( $1f_{7/2}^{\nu}, 1f_{7/2}^{\pi}$ ), ( $2p_{3/2}^{\nu}, 2p_{3/2}^{\pi}$ ) and ( $2p_{3/2}^{\nu}, 2p_{1/2}^{\pi}$ ) excitations. These particle-particle type excitations become possible only when  $T=1$  pairing interaction acts on the ground state. The occupation probabilities of neutron single particle states are obtained by integrating the lower components of HFB wave functions as  $v^2=0.69, 0.20, 0.10$  and  $0.08$  for  $1f_{7/2}, 2p_{3/2}, 2p_{1/2}$  and  $1f_{5/2}$  orbits, respectively. The proton states have almost the same occupation probabilities. With a strong  $T=0$  pairing ( $f=1.5$ ), the main configurations of the low energy peak become a coherent superposition of two quasi-particle (QP) excitations ( $2p_{3/2}^{\nu}, 2p_{1/2}^{\pi}$ ), ( $2p_{3/2}^{\nu}, 2p_{3/2}^{\pi}$ ), ( $1f_{7/2}^{\nu}, 1f_{5/2}^{\pi}$ ) and ( $1f_{7/2}^{\nu}, 1f_{7/2}^{\pi}$ ) as shown in Table 1. These coherent phases are inherent to the  $T=0$  pairing interaction and increases the GT strength. On the other hand, the higher energy peak is still dominated by the ( $1f_{7/2}^{\nu}, 1f_{5/2}^{\pi}$ ) configuration, but decreases its strength significantly.

The GT sum rule values  $S_{-}(GT)$  are given in Table 1 without and with the  $T=0$  pairing ( $f = 0.0$  and  $f = 1.5$ ). The  $S_{-}(GT)$  value is decreased when the  $T=0$  pairing is included [21]. This is due to the fact that the high excited GT strength is more decreased than the increase of the lower excited GT strength since the main configuration of GT strength ( $1f_{7/2}^{\nu}, 1f_{5/2}^{\pi}$ ) is hindered. The decrease of GT strength is always the case with  $T=0$  pairing also in the other  $N=Z$  nuclei studied in the present paper. The decrease of the  $S_{-}(GT)$  value is about 20% and going up to 30% in the cases of  $f = 1.5$  and  $f = 1.7$ , respectively. We have checked the increase of GT strength in the lower peak in  $^{56}\text{Ni}$  by using other Skyrme interactions SGII+Te1[24, 25], T43 and T32 [26]. We found that these features of GT states are robust with some minor differences in the excitation energy of two main peaks.

The enhancement of lower energy GT strength by the ( $T=0, S=1$ ) pairing can be induced by the transition between four QP states such as

$$\langle (j^2)_{S=0}^{T=1} (p_{3/2}^{\nu} p_{3/2}^{\pi})_{S=1}^{T_f=1} \| O(\hat{GT}) \| (j^2)_{S=0}^{T=1} (p_{3/2}^{\nu} p_{3/2}^{\pi})_{S=0}^{T=1} \rangle_{S_i=0}^{T_i=0} \\ = \langle (p_{3/2}^{\nu} p_{3/2}^{\pi})_{S=1}^{T=0} \| O(\hat{GT}) \| (p_{3/2}^{\nu} p_{3/2}^{\pi})_{S=0}^{T=1} \rangle \quad (6)$$

where the two quasi-particle configuration ( $j^2$ ) $^{T=1, S=0}$  (for examples,  $j = 1f_{7/2}^{\nu}$  or  $j = 2p_{3/2}^{\nu}$ ) acts as a spectator. The double bar in Eq. (6) is the symbol of doubly reduced matrix element both in spin and isospin space. Other QP configurations ( $1f_{7/2}^{\nu}, 1f_{7/2}^{\pi}$ ) $^{T=0, S=1}$ , ( $1f_{7/2}^{\nu}, 1f_{5/2}^{\pi}$ ) $^{T=0, S=1}$  and ( $2p_{3/2}^{\nu}, 2p_{1/2}^{\pi}$ ) $^{T=0, S=1}$  are also possible configurations in Eq. (6) equivalent to ( $2p_{3/2}^{\nu}, 2p_{3/2}^{\pi}$ ) $^{T=0, S=1}$ . It should be noticed that the  $T=1$  pairing works between the two particle configurations  $|(lj)^2 : (L = S = 0)J = 0, T = 1\rangle$  with  $j = 7/2, 5/2, 3/2$  and  $1/2$  in  $pf$  shell model space. On the other hand, the  $T=0$  pairing acts on the configurations  $|(lj, l'j') : (L = 0, S = 1)J = 1, T = 0\rangle$  with not only  $(l = l', j = j')$ , but also with  $(l = l', j = j' \pm 1)$ . This is the reason why the  $T=0$  pairing makes

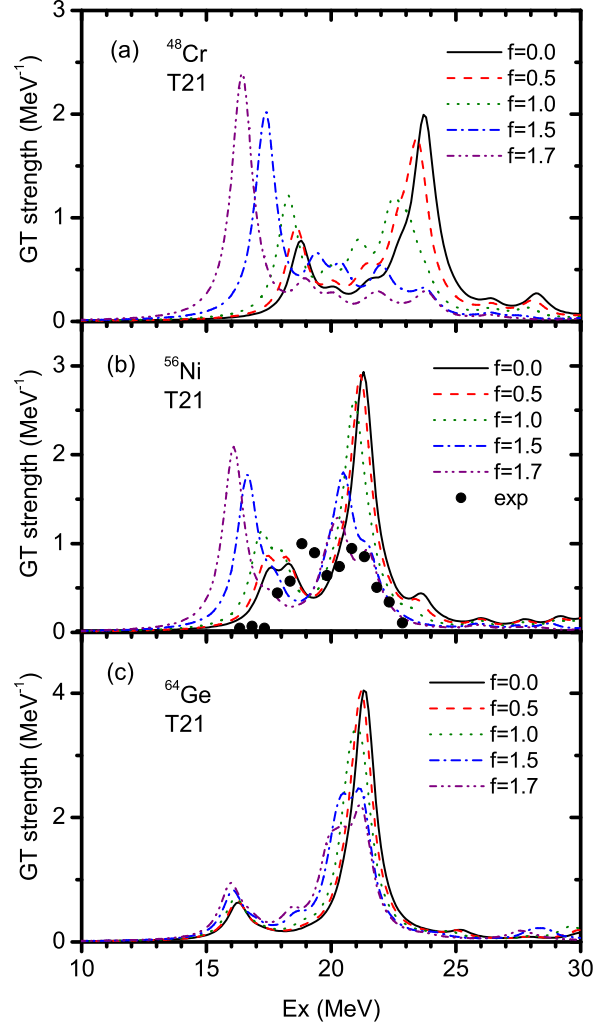


Figure 2: (Color online) Gamow-Teller strength in  $^{48}\text{Cr}$ ,  $^{56}\text{Ni}$  and  $^{64}\text{Ge}$  by HFB+QRPA with the Skyrme interaction T21. The quenching factor 0.74 is adopted for the GT transition operator  $\hat{O}(GT)$ . The  $T=0$  pairing interaction is included in QRPA calculations by changing the coupling constant from  $f=0.0, 0.5, 1.0, 1.5$  and  $1.7$  in Eq. (2). The experimental data of  $^{56}\text{Ni}$  are taken from Ref. [20].

strong couplings among ( $T=0, S=1$ ) pairs with ( $2p_{3/2}^{\nu}, 2p_{1/2}^{\pi}$ ) and ( $1f_{7/2}^{\nu}, 1f_{5/2}^{\pi}$ ) as well as ( $2p_{3/2}^{\nu}, 2p_{3/2}^{\pi}$ ) and ( $1f_{7/2}^{\nu}, 1f_{7/2}^{\pi}$ ), enhancing the lower energy GT peak in the case of  $f = 1.5$  in Table 1.

Main configurations of GT states in  $^{48}\text{Cr}$  and  $^{64}\text{Ge}$  are listed in Table 2 calculated with a strong  $T=0$  pairing ( $f = 1.5$ ). Because of partially occupied  $2p_{3/2}$ ,  $1f_{7/2}$  and  $1d_{3/2}$  orbits in  $^{48}\text{Cr}$ , the configurations ( $2p_{3/2}^{\nu}, 2p_{3/2}^{\pi}$ ), ( $1f_{7/2}^{\nu}, 1f_{7/2}^{\pi}$ ) and ( $1d_{3/2}^{\nu}, 1d_{3/2}^{\pi}$ ) give large contributions to the lower energy GT strength at  $E_x=17.4$  MeV having coherent phases. Although the high energy state at  $E_x=19.4$  MeV obtains large contributions from ( $2p_{3/2}^{\nu}, 2p_{3/2}^{\pi}$ ) and ( $1f_{7/2}^{\nu}, 1f_{5/2}^{\pi}$ ), it is cancelled by other configurations ( $1d_{3/2}^{\nu}, 1d_{3/2}^{\pi}$ ) and ( $1f_{7/2}^{\nu}, 1f_{7/2}^{\pi}$ ). This cancellation decreases substantially the  $B(GT)$  value compared with that of the state at  $E_x=17.4$  MeV. The situation is rather different in  $^{64}\text{Ge}$  since neutron and proton  $1f_{7/2}$  orbits are almost fully occupied. Thus the ( $1f_{7/2}^{\nu}, 1f_{7/2}^{\pi}$ ) configuration does not appear as a dominant configuration in the strong  $B(GT)$  states in Table

II. On the other hand, the  $2p_{1/2}$ ,  $2p_{3/2}$  orbits contribute significantly to the lower energy state at  $E_x=16.1$  MeV in  $^{64}\text{Ge}$ . The  $B(\text{GT})$  value of this state in  $^{64}\text{Ge}$  is only a half of the state at  $E_x=17.4$  MeV in  $^{48}\text{Cr}$  because of negligible contribution from the  $(1f'_{7/2}1f'_{7/2})$  configuration even though the  $T=0$  pairing is strong. The high energy state at  $E_x=21.2$  MeV in  $^{64}\text{Ge}$  is dominated by the  $(1f'_{7/2}1f'_{5/2})$  configuration, the same as the high energy state in  $^{56}\text{Ni}$ . The sum rule values  $S_-(\text{GT})$  of  $^{48}\text{Cr}$  and  $^{64}\text{Ge}$  are also given in Table 2 in the case of strong  $T=0$  pairing. In general, the sum rule value is larger for the heavier  $N=Z$  nuclei since available configuration space is larger. The increase of  $S_-(\text{GT})$  is 25% and 47% in  $^{56}\text{Ni}$  and  $^{64}\text{Ge}$ , respectively, in comparison with that of  $^{48}\text{Cr}$ .

Table 2: Same as Table 1, but for  $^{48}\text{Cr}$  and  $^{64}\text{Ge}$  with the  $T=0$  pairing interaction  $f = 1.5$ .

<sup>48</sup> Cr		<i>f</i> = 1.5			
E <sub><i>x</i></sub>	B(GT)	<i>ν</i> ( <i>v</i> <sub><i>ν</i></sub> <sup>2</sup> )	<i>π</i> ( <i>v</i> <sub><i>π</i></sub> <sup>2</sup> )	B	C
17.4	5.68	2p <sub>3/2</sub> (0.12)	2p <sub>3/2</sub> (0.12)	0.186	0.062
		1d <sub>3/2</sub> (0.85)	1d <sub>3/2</sub> (0.84)	0.251	0.204
		1f <sub>7/2</sub> (0.33)	1f <sub>5/2</sub> (0.07)	0.268	0.021
		1f <sub>7/2</sub> (0.33)	1f <sub>7/2</sub> (0.32)	1.04	0.558
19.4	1.19	2p <sub>3/2</sub> (0.12)	2p <sub>1/2</sub> (0.07)	0.215	0.081
		2p <sub>3/2</sub> (0.12)	2p <sub>3/2</sub> (0.12)	0.559	0.461
		1d <sub>3/2</sub> (0.85)	1d <sub>3/2</sub> (0.84)	−0.217	0.142
		1f <sub>7/2</sub> (0.33)	1f <sub>5/2</sub> (0.07)	0.383	0.038
		1f <sub>7/2</sub> (0.33)	1f <sub>7/2</sub> (0.32)	−0.384	0.054
S <sub>−</sub> (GT)=11.77					
<sup>64</sup> Ge		<i>f</i> = 1.5			
E <sub><i>x</i></sub>	B(GT)	<i>ν</i> ( <i>v</i> <sub><i>ν</i></sub> <sup>2</sup> )	<i>π</i> ( <i>v</i> <sub><i>π</i></sub> <sup>2</sup> )	B	C
16.1	2.15	2p <sub>3/2</sub> (0.48)	2p <sub>1/2</sub> (0.21)	−1.316	0.889
21.2	5.21	1f <sub>5/2</sub> (0.14)	1f <sub>7/2</sub> (0.90)	−0.187	0.353
		1f <sub>7/2</sub> (0.92)	1f <sub>5/2</sub> (0.15)	2.392	0.561
S <sub>−</sub> (GT)=17.26					

The peak ratio between GT strength of the low energy region (below  $E_x=20$  MeV) and the high energy region (above  $E_x=20$  MeV) is plotted in Fig. 3 as a function of mass number  $A$ . In the cases of weak  $T=0$  pairing ( $f \leq 1.0$ ), the high energy peak  $B_{\text{high}}(\text{GT})$  is larger than the low energy one  $B_{\text{low}}(\text{GT})$ . With stronger  $T=0$  pairing ( $f > 1.0$ ), the  $B_{\text{low}}(\text{GT})$  value becomes larger and dominates the GT strength distribution, especially in nuclei  $A \leq 56$ . The low energy peak may appear as a single giant resonance in the strong  $T=0$  pairing limit. The empirical ratio of  $B_{\text{low}}(\text{GT})$  to  $B_{\text{high}}(\text{GT})$  in  $^{56}\text{Ni}$  is obtained from observed

$B(\text{GT})$  strength distributions in Ref. [20]. The data point is consistent with the calculated ratio with the  $T=0$  pairing at  $f \sim 1.5$ .

The shell model calculations were performed for  $^{56}\text{Ni}$  by using effective interactions KB3G and GXPF1A in ref. [20, 27] and a particle-vibration coupling model is applied to calculate the GT strength in  $^{56}\text{Cu}$  in ref. [28]. The shell model interaction GXPF1A gives a two-peak structure for GT strength distributions. The competition between  $T=0$  pairing and the spin-orbit interaction may be a key issue of these results [27]. It is also shown in ref. [28] that the effect of particle-vibration coupling gives a sizable effect on GT strength distribution in  $^{56}\text{Cu}$  based on the HF+RPA model. It might be an interesting and challenging task to take into account the effect beyond HFB+QRPA such as the particle-vibration coupling effect in the microscopic model in future.

The strength of the  $T=0$  pairing can be determined by using the  $p$ - $n$  scattering length [29] in the same way as for the  $T=1$  pairing [30, 31]. The extracted value is slightly larger than the  $T=1$  pairing strength and, makes a bound deuteron state with a binding energy of 1.41 MeV, which is somewhat smaller than the experimental value 2.2 MeV. The effective density dependent pairing forces of zero range are obtained in  $T=0$  and 1 channels in symmetric nuclear matter from Paris forces in Ref. [14]. The obtained  $T=0$  interaction is much stronger than the  $T=1$  interaction. In Ref. [32], a phenomenological  $T=0$  pairing strength was determined to be 1.36 times stronger than the corresponding  $T=1$  pairing by fitting the ground state spins of several  $N=Z$  nuclei in the  $p$  shell region. The large value of the  $T=0$  pairing can be considered to mimic the effect of tensor correlations which contributes to the binding energy of deuteron significantly. At present, it is still an open question how much is the phenomenological  $T=0$  pairing interaction, which can be used for HFB and QRPA calculations in medium-heavy and also in heavy nuclei. As we have pointed out in this letter, the empirical data of GT strength in  $N=Z$  nuclei will provide important information to disentangle the  $T=0$  pairing in medium-heavy and heavy mass nuclei.

In summary, we study GT states in several  $N=Z$  nuclei in medium mass region by using HFB+QRPA model taking into account  $T=0$  pairing interaction. We found in the context of  $\text{SU}(4)$  supermultiplets that the low excitation energy GT strength is largely enhanced by  $T=0$  pairing interaction which is working cooperatively with the  $T=1$  pairing correlations in the ground state. Especially in the lighter nuclei  $N=Z=24\sim 28$ , the  $B_{\text{low}}(\text{GT})$  becomes comparable or even larger than the  $B_{\text{high}}(\text{GT})$  values in the strong  $T=0$  pairing ( $f \geq 1.0$ ). This enhancement of the lower energy GT strength is attributed to the coherent excitation of several  $pf$  shell configurations and can be considered as an implementation of the super-allowed GT transition in the  $\text{SU}(4)$  supermultiplets in the spin-isospin space. It is found that the available data in  $^{56}\text{Ni}$  is consistent with the calculated ratio  $B_{\text{low}}(\text{GT})/B_{\text{high}}(\text{GT})$  with the  $T=0$  pairing strength  $f \sim 1.5$ . Further additional information of empirical  $B(\text{GT})$  is desperately desired to confirm the role of  $T=0$  pairing in the GT states in  $N=Z$  nuclei.

We are grateful to Toshio Suzuki, M. Honma, M. Ichimura, K. Yako and T. Wakasa for valuable discussions. This work

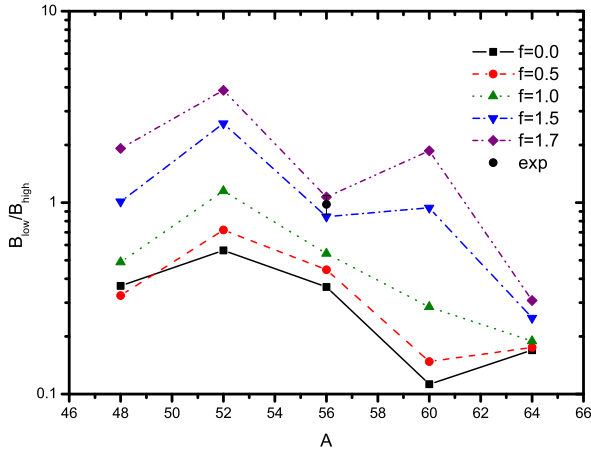


Figure 3: (Color online) Ratio between Gamow-Teller peaks in the lower energy and the higher energy regions as a function of the  $T=0$  strength parameter,  $f$ , calculated with T21 interaction. The lower energy and higher energy region is divided at  $E_x=20$  MeV. The experimental ratio in  $^{56}\text{Ni}$  is obtained from observed  $B(\text{GT})$  strengths in the lower and higher energy regions in Ref. [20].

is supported by the National Natural Science Foundation of China under Grant Nos. 10875172, 10275092, 10675169, and 11105094, and Financial Supports from Sichuan University (Project Nos. 2010SCU11086 and 2012SCU04A11). This work was also supported by the Japanese Ministry of Education, Culture, Sports, Science and Technology by Grant-in-Aid for Scientific Research under the program numbers (C) 22540262.

## References

- [1] A. Bohr, B. R. Mottelson, and D. Pines, Phys. Rev. **110**, 936 (1958).
- [2] A. Bohr and B. R. Mottelson, Nuclear Structure (Benjamin, New York, 1969) Vol. I.
- [3] D. M. Brink and R. Broglia, “*Nuclear superfluidity, pairing in Finite Systems*”, Cambridge monographs on particle physics, nuclear physics and cosmology, vol 24 (2005).
- [4] G. F. Bertsch, “*50 Years of Nuclear BCS*”, (World Scientific, edited by R. Broglia and V. Zelevinsky), arXiv:1203.5529v1 (March, 2012).
- [5] K. Matsuyanagi, N. Hinohara, and K. Sato, arXiv:1205.0078v1 (May, 2012).
- [6] M. Bender, P.-H. Heenen and P.-G. Reinhard, Rev. Mod. Phys. **75**, 121 (2003).
- [7] M. V. Stoitsov, J. Dobaczewski, W. Nazarewicz and P. Borycki, Int. J. Mass Spectrum, **251**, 243 (2006).
- [8] T. Duguet, P. Bonche, P.-H. Heenen, and J. Meyer, Phys. Rev. C **65**, 014311 (2001).
- [9] J. Margueron, H. Sagawa and K. Hagino, Phys. Rev. C **76**, 064316 (2007); Phys. Rev. C **77**, 054309 (2008).
- [10] J. Engel et al., Phys. Rev. C **60**, 014302 (2000).
- [11] M. Matsuo, Nucl. Phys. A **696**, 371 (2001).
- [12] E. Khan et al., Phys. Rev. C **66**, 024309 (2002).
- [13] N. Paar et al., Phys. Rev. C **67**, 034312 (2003).
- [14] E. Garrido et al., Phys. Rev. C **60**, 064312 (1999); E. Garrido et al., Phys. Rev. C **63**, 037304 (2001).
- [15] A. Poves, G. Martinez-Pinedo, Phys. Lett. B **430**, 203 (1998).
- [16] G.F. Bertsch and Y. Luo, Phys. Rev. C **81**, 064320 (2010), and references therein.
- [17] W. Satula, D. J. Dean, J. Gary, S. Mizutori and W. Nazarewicz, Phys. Lett. B **407**, 103 (1997).  
W. Satula and R. Wyss, Phys. Lett. B **393**, 1 (1997).

- [18] T. Wakasa et al., Phys. Rev. C **55**, 2909 (1997).  
M. Ichimura, H. Sakai and T. Wakasa, Prog. Part. Nucl. Phys. **56**, 446 (2006).
- [19] T. Suzuki, M. Honma, Hélène Mao, T. Otsuka and T. Kajino, Phys. Rev. C **83**, 044619 (2011).
- [20] M. Sasano et al., Phys. Rev. Lett. **107**, 202501 (2011).
- [21] E. Moya de Guerra et al., Nucl. Phys. A **727**, 3 (2003).
- [22] S. Fracasso and G. Colò, Phys. Rev. C **76**, 044307 (2007).
- [23] E. P. Wigner, Phys. Rev. **51**, 106 (1937); Phys. Rev. **56**, 519 (1939).  
F. Hund, Z. Physik **105**, 202 (1937).
- [24] C. L. Bai, H. Sagawa, H. Q. Zhang, X. Z. Zhang, G. Colò and F. R. Xu, Phys. Rev. C **79**, 041301(R) (2009); Phys. Lett. B **675**, 28 (2009).
- [25] C. L. Bai, H. Q. Zhang, X. Z. Zhang, F. R. Xu, H. Sagawa and G. Colò, Phys. Rev. Lett. **105**, 072501 (2010).
- [26] C. L. Bai, H. Q. Zhang, H. Sagawa, X. Z. Zhang, G. Colò and F. R. Xu, Phys. Rev. C **83**, 054316 (2011).
- [27] T. Lesinski, M. Bender, K. Bennaceur, T. Duguet, and J. Meyer, Phys. Rev. C **76**, 014312 (2007).
- [28] T. Suzuki and M. Honma, private communications.
- [29] Y. F. Niu, G. Colò, M. Brenna, B. F. Bortignon and J. Meng, Phys. Rev. C **85**, 034314 (2012).
- [30] E. Lomon and R. Wilson, Phys. Rev. C **9**, 1329 (1974).
- [31] G. F. Bertsch and H. Esbensen, Ann. Phys. (NY) **209**, 327 (1991).
- [32] H. Esbensen, G. F. Bertsch, and K. Hencken, Phys. Rev. C **56**, 3054 (1997).
- [33] N. Vinh Mau, arXiv:0711.3173v1 (Nov. 2007).